Cellulose (2022) 29:1435–1450
https://doi.org/10.1007/s10570-021-04365-w

ORIGINAL RESEARCH

A rheological study of cationic micro- and nanofibrillated cellulose: quaternization reaction optimization and fibril characteristic effects

Tilen Kopač · Matjaž Krajnc · Aleš Ručigaj

Received: 30 June 2021 / Accepted: 3 December 2021 / Published online: 4 January 2022

Abstract Driven by the demand for various cationic biopolymers in recent years, the quaternization of cellulose nanofibers was carefully investigated to have tight control over their final characteristics. The addition of sodium hydroxide (NaOH) to the reaction mixture is crucial as it catalyzes the conversion of alcohol groups of cellulose into more reactive alcoholate groups. On the other hand, excessive concentration proves to inhibit the reactivity of hydroxyl groups. The addition of glycidyltrimethylammonium chloride (GTMAC) increases the yield of the trimethylammonium chloride content (TMAC) reaction, while in excess it affects the rheological properties of the quaternizated cellulose nanofibers. The effects of NaOH and GTMAC on the TMAC content and rheological properties have been investigated in detail and mathematically evaluated. Furthermore, a comparison of the viscoelastic behavior and shear thinning character of commercial cationic micro- and nanofibrillated cellulose is presented. The research allows to extend the possibility of using cellulose in many applications of cationic biopolymers.

Keywords Cationic cellulose · Nanofibrils · Microfibrils · Rheology

T. Kopač · M. Krajnc · A. Ručigaj (✉)
Faculty of Chemistry and Chemical Technology, University of Ljubljana, Večna pot 113, SI-1000 Ljubljana, Slovenia
e-mail: ales.rucigaj@fkkt.uni-lj.si

Introduction

Biopolymers have become one of the most studied materials in recent decades, mainly due to their low toxicity, stability, biodegradability, resorbability, and renewable nature (George et al. 2020). These specific properties make biopolymers interesting in many promising industries, especially in the pharmaceutical, and medical fields (drug delivery systems (Jacob et al. 2018), tissue engineering (Velema and Kaplan 2006), regenerative medicine (Ebhodaghe 2020), cell implantation (Rebelo et al. 2017), biosensors (Tavakoli and Tang 2017), etc.). Among many natural biopolymers, cellulose, its derivatives (Ghorbani et al. 2018) and their modifications (Courtenay et al. 2018) have also proved useful in the mentioned areas. In addition to the characteristic properties of biopolymers listed above, cellulose has characteristics of biocompatibility, tunable functionality, mechanical strength, hydrophilicity, and relative thermal stability (Udoetok et al. 2016).

Cellulose is a linear polysaccharide composed of glucose residue monomers that are connected by β-(1-4)-glycosidic bonds (French 2017). The use of modified cellulose with different charges is of particular interest in the field of manufacturing gels for pharmaceutical (cosmetic) (Parhi 2017) and medical purposes (Caló and Khutoryanskiy 2015). Different charges on the surface (different functional groups) allow a wide range of applications of different crosslinking agents,

pH responsiveness to the environment, and electrostatic interactions between polymer chains (Ahmed 2015). The mechanical properties of the hydrogel structure can be determined by rheological measurements. The presence of three hydroxyl groups contributes to the formation of intra- and intermolecular hydrogen bonds, which determine the most important chemical and mechanical properties of cellulose-based materials (John and Thomas 2008). At a concentration above 1 wt%, the cellulose-based materials can form strong gels with highly entangled networks in water (Šebenik et al. 2019). Besides, the rheological properties of hydrogels are influenced by morphology (fiber or particle size, its shape and distribution) (Colson et al. 2016), in addition to the different content of surface charge, hydrogen bonds, and electrostatic interactions (Kopač et al. 2021). Depending on the particle size we distinguish between microfibrillated (CMF) and nanofibrillated (CNF) cellulose. The main difference between CMFs and CNFs is their diameter (Zhang et al. 2012). The size distribution of the CMF fibers is wide, and even if some fibers have diameters in the nanometer range, at least one dimension of fibers is in the micrometer range (more details in Materials). The structure consists of long and thin fibers that are interconnected in a network structure (Turpeinen et al. 2020). CMFs have a viscoelastic and shear thinning behavior (Iotti et al. 2011; Schenker et al. 2019), but a higher viscosity and critical stress than CNFs (Moberg et al. 2017). On the other hand, the CNF diameter never exceeds 100 nm (see section Materials). Compared to the CMFs, the diameter is smaller, the surface charge is much higher, it binds more water, and has a higher degree of swelling. Consequently, CNFs can build up a typical hydrogel structure at lower concentrations (Dimic-Misic et al. 2013). From the listed differences between CMFs and CNFs, significant differences in rheological properties can be expected, especially when compared to different concentrations of positive charge groups on the surface.

Among other properties, biopolymers with different surface charges are needed, especially in drug delivery systems (Li and Mooney 2016). Therefore, various modifications of biopolymers have already been made in research over the last decade. The number of anionic biopolymers (Gasperini et al. 2014) is much higher than the number of cationic biopolymers (Samal et al. 2012). Even in the case of cellulose, the modification of cellulose into an anionic form has already been well researched. Furthermore, the TEMPO oxidation of cellulose (Isogai et al. 2011) nanofibrils is also available in the commercial form (Kopač et al. 2020). On the other hand, the demand for cationic biopolymers is also high, but most industrial products focus only on the use of chitosan (Ahmadi et al. 2015). In recent years, numerous other modifications of cationic biopolymers have been developed (Samal et al. 2012; Farshbaf et al. 2017). The same applies for the cationic functionalization of cellulose, in which the modification of cellulose with epichlorohydrin-ammonia reaction (Spaic et al. 2014) and the grafting with quaternary ammonium salts (quaternization of cellulose) (Hasani et al. 2008; Zaman et al. 2012; Salajková et al. 2012; Chaker and Boufi 2015) predominate.

In the present study, both modifications were tested, whereby significantly higher reaction efficiencies were achieved by the quaternization of cellulose (epichlorohydrin may enhance the surface area, porosity and hydrophobic character of the hydrogel (Udoetok et al. 2016)). Furthermore, it was found out that the control of the concentration of reactants during this reaction allows the design of the product with different rheological properties that can be used in a variety of applications. The influence of reaction parameters in the modification process on the rheological properties of the final product was investigated summed up in a mathematical model for easy control of the desired end product properties. It was hypothesized that the optimal catalyst concentration (NaOH) in quaternization of nanofibrillated cellulose is crucial in control designing of a biopolymer with the desired content of cationic groups on the surface, which predominantly influence the targeted rheological properties of the product. Furthermore, the effect of cationic cellulose fiber size (micro- and nanofibers) on the shear thinning character and viscoelastic properties was investigated. Rheology provides insight into the internal structure of hydrogels and evaluates the predominant interactions that construct the hydrogel network. Flow properties, zero-shear rate viscosity, and critical stress data allow the selection of a suitable hydrogel application, while mechanical properties with shear modulus information are used to design hydrogels as drug delivery systems in controlled release technology (Kopač et al. 2020).

Experimental

Materials

Cationic microfibrillated cellulose (CCMF), dispersion of pulp, cellulose 2-hydroxy-3-trimethylammonium chloride propyl ether in water was purchased from Weidmann Fiber Technology by Weidmann Electrical Technology Ag, Switzerland. According to specifications given by the producer, the solids content was adjusted to 2.6 wt% and the CCMF structure is branched, with particle length (D_{50}) of 7-11 µm (method of determination was ISO 13322-2:2006-11).

Cationic cellulose nanofibrils (CCNFs) were supplied by Cellulose Lab, Canada. According to specifications given by the producer, the slurry product was prepared by high pressure homogenizer (nano-fibrillation of pulp fiber to CNFs). The solid content was adjusted to 3 wt%. The CCNFs possess quaternary ammonium surface groups with a charge density of 2.4 meq/g (which is equal to 2.4 mmol/g TMAC). The structure is forked with dimensions of 50 nm in width and lengths of up to several hundred microns.

Freeze-dried cellulose nanofibers (CNFs), made from wood pulp were purchased from The Process Development Centre, University of Maine (UMaine PDC), USA. The surface was unmodified with fiber dimensions of 20–50 nm in width and lengths of up to several hundred microns.

N,N-Dimethylacetamide (DMAC), glycidyltrimethylammonium chloride (GTMAC), sodium hydroxide (NaOH), and silver nitrate ($AgNO_3$) were used as received from Sigma-Aldrich (St. Louis, USA).

Quaternization of cellulose nanofibers

The CNFs were purified four times in water and collected each time by centrifugation (Colo Lace16R) for 10 min at 10,000 rpm. In order to prevent agglomeration of the fibers, to achieve stronger interaction with the solvent, efficient swelling of the fibers, and good accessibility of the reagent to the inner pore, the CNF fibers were soaked in distilled water overnight (Chaker and Boufi 2015). The water was then removed by centrifugation and washed twice with DMAC. Water was removed to avoid hydrolysis of GTMAC and degradation of cationic CNFs during synthesis (Zaman et al. 2012). The CNF fibers were then dispersed (dry powder content of 1.4 wt%) in DMAC (water was replaced by DMAC to limit hydrolysis of the epoxy ring during the reaction) using a WiseTis homogeniser. In addition to DMAC, the continuous phase also contained NaOH in different molar ratios depending on the amount of CNFs (the amounts are shown in Fig. 1). NaOH catalyzes the conversion of alcohol groups of cellulose into more reactive alcoholate groups (Ho et al. 2011). In this way, the efficiency of the modification is increased, however, an excessive concentration of NaOH inhibits the modification of reactive hydroxyl groups. The dispersion was transferred to a reactor vessel in which a temperature of 65 °C was maintained on a propeller stirrer with constant stirring at 500 rpm. When the reactor mixture reached the reaction temperature, GTMAC (which was selected as the cationization agent due to its high cationization efficiency (Zaman et al. 2012)) was added in different molar ratios relative to the added cellulose (molar ratio GTMAC/CNFs in Table 1). After 24 h, the reactor mixture was centrifuged and purified with water until all DMAC and unreacted GTMAC were washed. The reaction product is surface quaternized cellulose nanofibers (QCNFs).

Characterization

Fourier transform infrared (FTIR) spectroscopy

The FTIR spectrum was performed to identify the different bonds present in cellulose samples and to demonstrate the successful covalent coupling of glycidyltrimethylammonium chloride to cellulose. Samples of CCNFs, CCMFs, and QCNFs were dried in a vacuum oven Kambič VS-50 SC at 25 °C and 0 bar until a constant weight was achieved. The FTIR was performed at IR Spectrometer Bruker FTIR Alpha Platinum ATR.

Raman spectroscopy

Raman spectroscopy was done on a Raman/AFM WITec Alpha 300RA instrument with green laser emitting light at 532 nm and intensity of 20 mW+. The integration time was 2 s. The same preparation of samples as in 2.3.1. was performed.

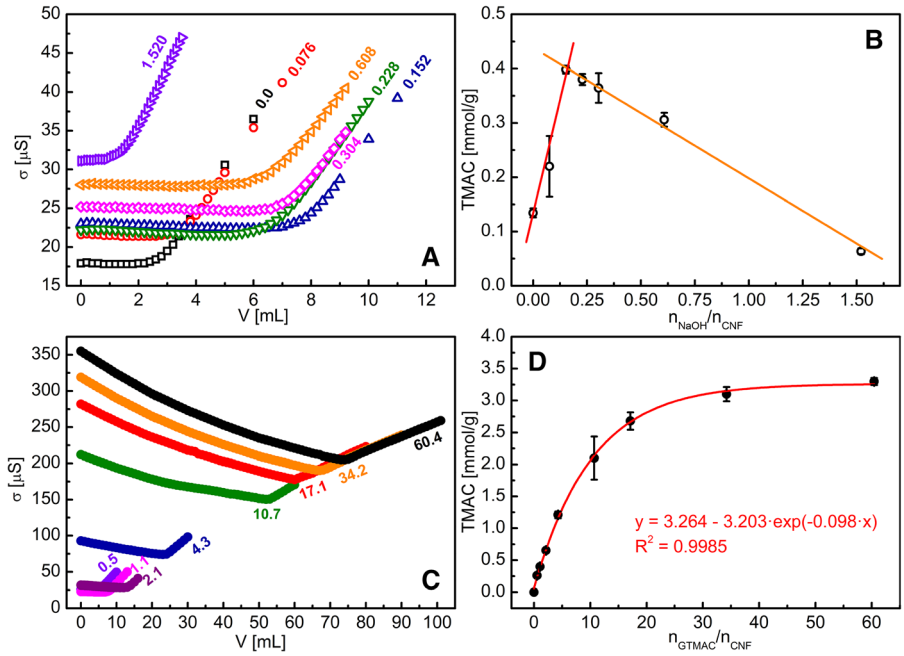

Fig. 1 Conductometric titration curves and the calculated values of TMAC as a function of NaOH (**A**, **B**) and GTMAC (**C**, **D**). The colors and symbols represent the various additives of corresponded reactant which is enriched with the numbers (ratio of molar amount of NaOH or GTMAC on the molar amount of CNFs in the reaction mixture)

Table 1 Fitting parameters values of zero-shear rate viscosity η_0, critical stress σ_c and shear moduli G for 2 wt% QCNF hydrogels synthesized by different concentrations of GTMAC

Polymer system	n_{GTMAC}/n_{CNF}	η_0 [Pa·s]·10^{-5}	σ_c [Pa]	G [Pa]	TMAC [mmol/g]
2 wt% QCNF	0.5	13.5	103	679	0.26
(n_{NaOH}/n_{CNF} = *0.152*)	1.0	8.05	101	739	0.40
	2.0	7.75	78.5	723	0.65
	4.0	7.57	76.1	650	1.21
	11	7.12	35.7	531	2.10
	17	3.79	23.9	528	2.68
	34	2.20	17.3	172	3.10
	60	1.03	7.94	141	3.30

The TMAC content determined by conductometric titration is also attached.

Scanning electron microscopy (SEM) studies

Morphology of cellulose materials was analyzed by scanning electron microscopy (SEM) using a FE-SEM ULTRA Plus (Carl Zeiss, Oberkochen, Germany) instrument. Before SEM analysis the 0.01wt% dispersion of biopolymers was sparsely sprinkled onto a silicon wafer tape attached to metal stubs and then dried in a vacuum oven Kambič VS-50 SC at 25 °C and 0 bar. The samples were imaged using an accelerating voltage of 1 kV under vacuum conditions (SE2 detector).

Zeta potential

The zeta potential (ζ) measurements were measured by ZetaSizer Nano ZS (Malvern Instruments). In this case, a 0.04 wt% dispersions of biopolymers were

prepared in deionized water. The dispersions were pretreated with ultrasonication using handheld ultrasonic homogenizer Hielscher UP200Ht with a 10 mm sonotrode at 40 W/cm^2 power output using 1 s on/off pulses for 2 min to break aggregates, so the charge hold together in a relatively individualized form within a stable dispersion. The zeta potential ζ was determined by the Helmholtz-Smoluchowski equation (Kaneko et al. 2010).

Conductometric titration

The trimethylammonium chloride (TMAC) content was determined by measuring the conductivity of the dispersion of the sample under investigation (100 mg dried sample of QCNFs, CCNFs, and CCMFs were dispersed in 100 mL Milli-Q water) as a function of the addition of a volume of 5 mM $AgNO_3$ solution on a Knick Portamess conductometer. The result is a curve with two characteristic phases: (1) Titration of chloride ions on TMAC with silver ions in an equivalent molar ratio - the conductivity remained approximately constant until (2) The molar amount of Ag^+ exceeds the molar amount of Cl^- (precipitation with a characteristic linear increase in conductivity). The TMAC content [mmol/g] was determined as the molar amount of Ag^+ ions (product of known concentration and the volume of $AgNO_3$ consumed in the first stage - an equivalent molar ratio to chloride ions on TMAC) per gram of dried QCNFs.

Rheological measurements

The effect of the addition of NaOH and GTMAC during the quaternization reaction of cellulose nanofibers on the rheological properties of QCNF hydrogels was investigated. Additionally, the influence of the cationic cellulose hydrogel concentration (1-3 wt%) on the pseudoplastic and thixotropic properties was studied. Consequently, the differences between the rheological properties of cellulose micro- and nanofiber hydrogels were carefully investigated. To perform rheological measurements, the 2 wt% QCNF dispersion was prepared by homogenizing the dried powder in distilled water. The CCNF and CCMF hydrogels were prepared in different concentrations of 1 to 3 wt% by diluting the original dispersion with distilled water. In order to obtain a hydrogel structure, the dispersions were pretreated with ultrasonication using handheld ultrasonic homogenizer Hielscher UP200Ht with a 10 mm sonotrode at 40 W/cm^2 power output using 1 s on/off pulses for 2 min (until the dispersion turned into a stable gel –the effect of sonication (time) of cellulose nanofiber on rheological properties is shown elsewhere (Lee et al. 2020)). The samples were then stored for 24 h at 4 °C to obtain the final hydrogel structure.

Oscillation and rotation tests were performed on the rheometer Anton Paar Physica MCR 301, equipped with a hatched plate with 50 mm diameter (PP50/P2), at a temperature of 25 °C. The frequency tests were performed within the linear viscoelastic range (at a constant strain of 0.1%, determined by amplitude tests) at the oscillation frequencies of 100 to 0.01 Hz. The results of the frequency tests (mechanical spectra) are plots of storage (G') and the loss module (G'') against the pulsation ω (=2$\pi\nu$). For a detailed discussion of the linear viscoelastic behavior of samples, the results were fitted with the classical generalized Maxwell model (Maxwell-Wiechert model), which consists of the equilibrium modulus of the elements G_e and Maxwell elements G_i (relaxation modules). According to the storage and loss modulus, the shear modulus (G) is estimated from the sum of the elastic Maxwell elements.

Flow curve – viscosity was measured over the range of shear stresses from 0.1 to 200 Pa. For a detailed investigation of the shear thinning character of samples, the zero-shear rate viscosity (η_0), critical stress (σ_c), and infinite-shear rate viscosity (η_∞) must be known. Therefore, the experimental flow curves were fitted by the Roberts-Barnes-Carew (RBC) model, which is the modified original Ellis equation. All the equations mentioned and the exact procedures for fitting the results of frequency and flow-viscosity tests are clearly described in our previous paper (Šebenik et al. 2019, 2020; Kopač et al. 2020).

Particle size analysis

The number particle size distribution was determined using a laser diffraction particle size analyzer Microtrac S3500 Bluewave. The samples were measured in three sequentially performed runs, from which averages were calculated and used in the data analysis.

Results and discussion

Control of quaternization of cellulose nanofibers and their structural properties depending on the target application

The key parameters in the quaternization of cellulose nanofibers are the concentration of NaOH and GTMAC. The concentration of trimethylammonium chloride (TMAC), which is modified on the surface of cellulose nanofibers (QCNFs), was determined by conductometric titration (Fig. 1 A and C). The method was verified by the CCNF sample measurement, where almost the same amount of TMAC content value was determined (Table 2) as specified by the producer (see Materials).

Figure 1 A reports on the results of the conductometric curves of QCNF samples with different NaOH additions at constant GTMAC concentration ($n_{GTMAC} = n_{CNF}$). The TMAC content on the surface of modified QCNFs is shown in Fig. 1B (see calculation from section Conductometric titration). NaOH acts as a catalyst since QCNF functionalization with TMAC is successful even at NaOH-free synthesis. NaOH catalyzes the conversion of alcohol groups of cellulose into more reactive alcoholate groups (Ho et al. 2011). Figure 1B shows the maximum quaternization efficiency of cellulose nanofibers at the molar ratio of 0.152 NaOH per molar quantity of CNFs (n_{NaOH}/n_{CNF}). Obviously, an excessive concentration of NaOH inhibits the modification of reactive hydroxyl groups, which could be explained by different polymorphic crystal structures of cellulose (I-IV). Cellulose I exists as a crystalline structure of natural cellulose. In addition, under the influence of aqueous sodium hydroxide solution, it penetrates into amorphous areas and with increasing concentration, leads to water binding and swelling. The polymer chains in these swollen areas are more mobile and can diffuse laterally to form an alkali complex. The increase in alkali concentration then allows penetration into the crystalline regions (Budtova and Navard 2016). The result is a change in the dimension of the basic elementary cell and the formation of cellulose II. Furthermore, cellulose III and cellulose IV exist as modified cellulose from cellulose I. Many possible hydrogen interactions between cellulose are the reason for the higher thermodynamic stability of type II-IV and the irreversibility of the reconversion into cellulose I (Mittal et al. 2011). To conclude, the optimal NaOH concentration in quaternization of cellulose nanofibers has to be determined.

Next, the effect of GTMAC concentration on TMAC content at an optimal concentration of NaOH (0.152 of n_{NaOH}/n_{CNF}) is shown in Fig. 1 C and D. The increased addition of GTMAC to the reaction mixture increases the TMAC content on the surface of cellulose nanofibers (Fig. 1D; Table 1). Theoretically, when all reactive hydroxyl groups are converted to TMAC, the highest concentration that can be achieved by the quaternization reaction is 4.2 mmol/g (calculated from literature (Ho et al. 2011)). It has to be noted that a theoretical value, based on the radius (average value) of the fibrils without taking into

Table 2 Fitting parameters values of zero-shear rate viscosity η_0, critical stress σ_c and shear moduli G for 1–3 wt% hydrogels based on cationic microfibrillated (CCMF) and nanofibrillated (CCNF) cellulose

Polymer system	Concentration [wt%]	η_0 [Pa·s]·10^{-5}	σ_c [Pa]	G [Pa]	TMAC [mmol/g]
CCMF	1.0	0.73	6.08	143	0.63
	1.5	2.08	7.81	182	
	2.0	8.85	36.2	682	
	2.5	12.1	48.4	793	
CCNF	1.0	0.66	8.81	98.5	2.24
	1.5	1.30	18.1	188	
	2.0	2.06	22.4	307	
	2.5	3.23	36.9	424	
	3.0	4.58	37.1	522	

The TMAC content determined by conductometric titration is also attached.

account the surface of the outermost cellulose chains, may be inaccurate due to possible radii variation. On the other hand, Fig. 1D shows that the upper limit of the nanocellulose functionalized TMAC concentration has been reached at 3.3 mmol/g, which is, according to the literature, the highest concentration of TMAC reached so far. The high reaction efficiency in comparison to other studies is due to the optimized concentration of the NaOH catalyst in the reaction mixture. Later in the discussion, it was also found that the TMAC concentration significantly influences the interactions between the polymer chains as well as the water molecules when swelling in the aqueous QCNF dispersion, which consequently has an influence on the rheological properties of the product (Fig. 3). Depending on the application, the requirements for different rheological properties vary. The experimental data in Fig. 1D were fitted with the exponential function. With Eq. (1), the properties of the final product can be easily controlled (during the synthesis) according to the desired application:

$$TMAC\left[\frac{mmol}{g}\right] = 3.264 - 3.203 \cdot \exp\left(-0.098 \cdot \frac{\eta_{GTMAC}}{\eta_{CNF}}\right) \quad (1)$$

where the concentration of the cationic groups is the molar amount of TMAC in 1 g of cellulose nanofibers [mmol/g] and the n_{GTMAC} and n_{CNF} is the molar amount of GTMAC and CNFs, respectively [mol]. The equation was developed based on the NaOH addition of 0.152 $n_{\mathrm{NaOH}}/n_{\mathrm{CNF}}$.

To highlight the quaternization of the cellulose nanofibers, in Fig. 2 A is presented the FTIR spectra of the unmodified CNFs, cationically modified CCNFs, CCMFs (commercial form) and cationically synthesized QCNFs (all spectra of modified QCNF samples reported peaks at the same wavenumbers, so only one sample is shown in Fig. 2 A). A strong band due to hydroxyl (–OH) stretching appeared at 3320 cm^{-1} (Nastaj et al. 2016; Lungu et al. 2021). At 2880 cm^{-1} there are the vibration bands of symmetric C–H groups (Nastaj et al. 2016; Siqueira et al. 2019). A mild band at 1630 cm^{-1} originated from the absorbed moisture (Zaman et al. 2012). The bands at 1300 cm^{-1} are attributed to the C–O stretching vibration (Nastaj et al. 2016). The next peak, between 1150 cm^{-1} and 1050 cm^{-1} is related to C–O and C–C stretching in major ether bands (Zaman et al. 2012; Lungu et al. 2021). The band around 1050 cm^{-1} also corresponds to the pyranose ring ether band of cellulose (Salajková et al. 2012). The absorption band at 900 cm^{-1} can be assigned to the C–H deformation mode of the glycosidic linkage between the glucose units which is attributed to the polysaccharide structure of cellulose (Zaman et al. 2012; Siqueira et al. 2019). These peaks are presented in all cellulose types, while a new peak appeared at 1480 cm^{-1} only in CCMF, CCNF, and QCNF samples, corresponding to the CH_2 bending mode and methyl groups of the cationic substituent (TMAC content). On the other hand, for CNFs the peak at 1480 cm^{-1} is absent, which proves the successful ionic exchange of quaternary ammonium salt (Zaman et al. 2012; Salajková et al. 2012). Furthermore, Fig. 2B displays the Raman spectra of CNF, CCMF, CCNF and QCNF samples. The Raman spectrum shows several distinct sharp bonds that can be

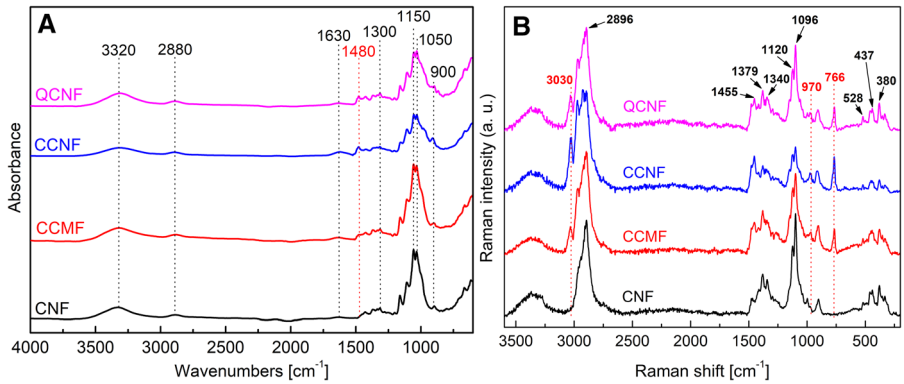

Fig. 2 FTIR spectra **A** and Raman spectra **B** of un-modified CNFs and cationically modified CCMFs, CCNFs (commercial form) and synthesized QCNFs

assigned to the structural properties of cellulose. The band at 2896 cm^{-1} is due to the CH stretching vibrations. Also, the corresponding CH deformation bands are observed in the fingerprint region at 1455, 1379 and 1340 cm^{-1}. The C–OH stretching vibrations can be observed at 1120 cm^{-1}, while the band at 1096 is assigned to the C–O–C stretching vibration of the α-glucose ring. The peaks at 528, 437 and 380 cm^{-1} are assigned to the skeletal mode involving the C–O–C ring mode. However, for cationically modified cellulose (CCMFs, CCNFs, and QCNFs), the expected bands of the trimethylammonium group $(CH_3)_3\ N^+$ can be observed at 3030, 970, and 766 cm^{-1} (indicated as red in Fig. 2B).

The small amount of QCNFs well dispersed in water has very promising rheological properties, which extend over several orders of magnitude making it very interesting to be used in many applications of QCNF based hydrogels. The rheological properties of 2 wt% QCNF hydrogels with different content of cationic TMAC groups on the CNF surface (Fig. 1D) are shown in Fig. 3. Flow curves with shear thinning behavior are illustrated in Fig. 3A, where the increase of shear thinning character with the increased concentration of GTMAC is evident. With lower GTMAC additions, the hydrogels behave more plastic (higher zero-shear rate viscosity, see Table 1), while with higher addition of GTMAC, a significant viscosity decrease in a narrow stress interval increases, which exhibits a typical characteristic of pseudoplastic fluids (Tang et al. 2018). In this case, critical stresses occur much earlier (Table 1). For GTMAC additives in a molar ratio of 17 or more relative to the molar amount of CNFs, the formation of a 2nd Newtonian plateau could be observed. In Fig. 3, it is shown that the samples "creep" and plastically deform even under conditions of very low shear stresses. Nevertheless, their viscosity is very high (due to a strong internal structure) until the critical stress is reached. This is followed by the rotation of the dispersed building blocks/clusters in the direction of the shear force, which then at high shear stress form a new hydrogel structure more liquid-like character. On the other hand, in hydrogels with a lower addition of GTMAC (up to 17 n_{GTMAC}/n_{CNF}), the decay of the hydrogel structure with irreversible return occurs when the critical shear stress is exceeded. This proves that the mechanical stress and swelling properties of cationic hydrogels are strongly dependent on the content of TMAC in the network. In cellulose hydrogels without additional crosslinking, the 3D structure (clusters formation (Šebenik et al. 2019)) is mainly formed by hydrogen bonds between hydroxyl groups, van der Waals forces, and electrostatic repulsion (Kopač et al. 2021), which is reinforced by functionalization of the cellulose surface with TMAC groups. The presence of positive charges (cationic TMAC) expanded the hydrogel network and improved the swelling ratio (Peng et al. 2016), which increased shear thinning in viscoelastic behavior. The cation-cation electrostatic repulsion in the hydrogel network led to the increased osmotic pressure of the fibers (difference in ionic concentration between the interior and the exterior of the fibers), which reduced the hydrogen interaction, thus increasing the distance between the fibrils. This allows the diffusion of water into the inner structure of the hydrogel (swelling) (Chaker and Boufi 2015). The direct dependence of TMAC content on electrostatic interactions that formulate the hydrogel structure is demonstrated by the almost linear drop of TMAC on critical stress (Table 1). In addition, Fig. 3B reports the mechanical spectra of 2 wt% QCNF hydrogels with different TMAC contents (additions of GTMAC) where the *G*' is higher than the *G*'' within all the angular frequency range with only slightly dependent *G*' and *G*'' evidencing a gel-like behavior. At higher GTMAC concentrations (more TMAC) the storage modules are the lowest and vice versa. As already mentioned,

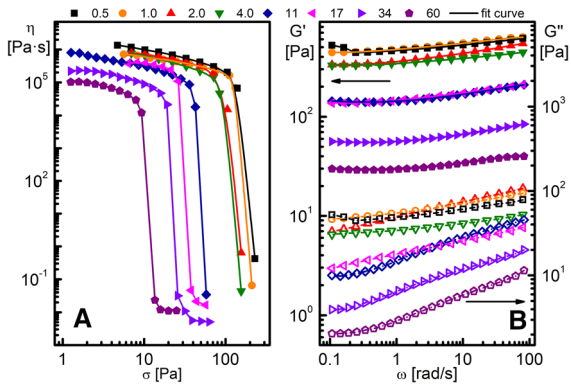

Fig. 3 Flow curves **A** and frequency dependence **B** of viscoelastic moduli (G'-filled symbols, G''-corresponding empty symbols) for hydrogels based on quaternized cellulose nanofibers of different GTMAC molar ratio to CNFs (numbers in legend) and constant NaOH addition (0.152 of n_{NaOH}/n_{CNF}) during synthesis

higher TMAC contents are involved in a higher electrostatic interaction (lower hydrogen interaction), which allows for a higher swelling ratio and is resulted in lower storage moduli. Furthermore, the higher slope of the elastic modules also contributed to the less stable network structures.

Rheological properties of cationic microfibrillated and nanofibrillated cellulose

The influence of the number of cationic groups on the mechanical properties of hydrogel has been discussed in previous section. Here, to further prove the cationic cellulose usability, the focus is on the effects of the fibrils dimension (nano vs. micro) of commercially available cellulose on the rheological properties. Figure 4A and C illustrate the rheological properties of CCNF hydrogels, and Fig. 4B and D show CCMF hydrogels characteristics. Mechanical spectra (Fig. 4A and B) report an increase in *G*' and *G*'' with cellulose fibril concentration. The ratio between *G*'' and *G*' is between 0.1 and 0.25 for all concentrations in the entire frequency range (similar results are shown in (Agoda-Tandjawa et al. 2010) where the native cellulose microfibrils was tested) and *G*' is almost independent of frequency (Šebenik et al. 2020), which means that the medium is structured in the same way, resulting in a gel-like structure. The shear thinning properties are evident from Fig. 4 C and D. Plastic behavior, higher zero-shear rate viscosity, and higher critical stress values become more significant with higher concentrations of cellulose fibrils. The significant viscosity decrease, limited in a narrow stress interval, is obvious for all samples that possess at least a slight 2nd Newtonian plateau, typical for weak polymer gels. Table 2 reports on the fitting parameters of the experimental data in Fig. 4, showing a wide interval of zero-shear rate viscosity and critical stress. Furthermore, the low values of shear modulus typical for gels without addition of crosslinking agents (weaker hydrogel structures) are obvious.

A comparison of the flow curves (Fig. 4 C and D) between CCNFs and CCMFs shows that the CCMFs reflect a slightly higher zero-shear rate viscosity. Fibrils in the aqueous dispersion form invisibly small clusters with swelling ability in water resulting from the intertwining of non-covalent and covalent

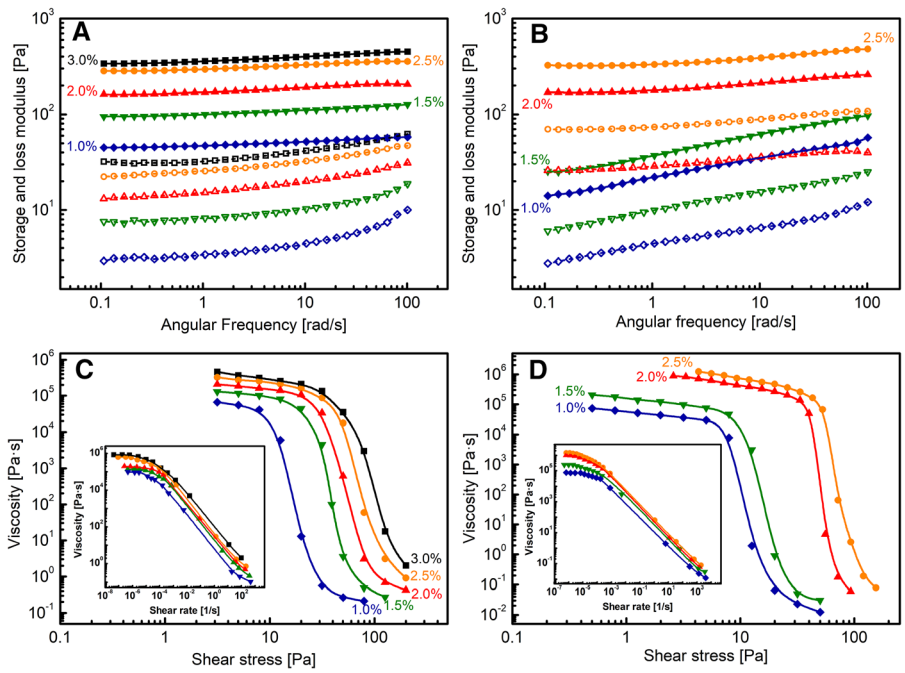

Fig. 4 Mechanical spectra (**A**, **B**) with G'-filled symbols, G''-corresponding empty symbols and flow curves (**C**, **D**) of 1–3 wt% hydrogels based on cationic cellulose fibers of different dimensions: A, C and B, D correspond to nanofibrillated (CCNF) and microfibrillated (CCMF) hydrogels, respectively

interactions between them (Šebenik et al. 2019). The electrostatic repulsion in this case should also be identified, as explained in detail in Sect. 3.1. Due to the larger dimension of the CCMFs, the resulting clusters or flocs become larger, which reduces the distance between them and leads to more hydrodynamic and non-covalent interactions among them. The consequence is higher zero-shear viscosities of the CCMFs compared to CCNFs at the same biopolymer concentrations (Table 2). On the other hand, the mechanical stability of the CCMF hydrogels is very interesting. Figure 4B shows that CCMFs form a weak structure at concentrations of 1.0 and 1.5 wt% (higher slope of the frequency-dependent *G*' and *G*'' curves). Figure 4D shows an even more drastic increase in critical stress and zero-shear rate viscosity between 1.5 and 2.0 wt% biopolymer concentration. This may be due to lower TMAC contents on the CCMF surface than prescribed on the CCNFs. As a result, there is less electrostatic interaction between polymer chains and a lower swelling ratio. Due to the low TMAC concentration, the CCMFs require a higher concentration of the biopolymer in the dispersion to form a stable hydrogel structure. On the other hand, stable CCNF hydrogel structure can already be seen at 1 wt%. Therefore, it is reasonable to compare CCNFs and CCMFs only in the stable area of the hydrogel structure above 2 wt%. CCMFs express higher critical stresses and higher shear moduli in this region due to larger clusters. Shear moduli are inversely proportional to pore size in the hydrogel network, which can be very useful for the hydrogel design for the targeted drug delivery in control release technology (Kopač et al. 2020). In comparison to shear moduli (Table 2), CCMFs have a smaller mesh size, but on the other hand, on CCNF hydrogel it is more easily control pore size by crosslinking due to their significantly higher TMAC content. The use of CCMFs or CCNFs depending on the rheological properties is, therefore, application dependent.

The effect of morphology of raw cellulose material on the final properties

The rheological properties of cationic cellulose micro/nanofibers are well discussed in previous sections. In Fig. 3 (see also Table 1) the shear-thinning character and viscoelastic behavior of dispersions decreases with TMA content on the surface of biopolymer (QCNFs). In Fig. 4 (see also Table 2) the effect of size dimensions of cellulose fibers (micro or nano dimensions) and biopolymer concentration on shear-thinning character and viscoelastic behavior is presented. Furthermore, as shown in Tables 1 and 2, the 2 wt% QCNFs with 2.1 mmol/g of TMAC on the surface of biopolymer shows different results from that of 2 wt% CCNFs with TMAC 2.24 mmol/g, even though they have similar TMAC and hydrogel concentration (see rheological properties summarized in Fig. 7 A and B). At this point, it is necessary to analyze the morphology of cellulose materials and to examine the aspect ratio and size distribution which can be different between starting materials. Therefore, the SEM analysis (Fig. 5), zeta potential measurements (Fig. 6) and particle size analysis (Fig. 7 C and D) were performed.

The SEM micrograph of CNF, CCMF, CCNF and QCNF biopolymers are presented in Fig. 5. The individual fibrils can be clearly detected in the CNF micrograph where the mixed sizes of long fibrils (dimensions of 20–50 nm in width and lengths of up to several hundred microns) and fibril bundles that have a high aspect ratio (which greatly exceeding 100) are evident. Furthermore, the highly complex network structures, rather than individual fibrils, can be observed in CCMF, CCNF and QCNF micrograph. The images show agglomeration of the nano/microfibrils of cellulose due to the hydrogen bonds formed after mechanical defibrillation (the CNFs develop floc structures during suspension stirring in case of highly charged surfaces (Šebenik et al. 2019)) or during the quaternization process (QCNFs), where a network of fibrils and larger expanded fibrillar aggregates are developed. Finally, the CCMF micrograph shows the cellulose microfibrils with the ability to agglomerate to each other. In addition, microcracks can also be observed in this case. The SEM analysis shows a high aspect ratio for cellulose fibrils which, in addition to charged nature of fibrillated cellulose, gives rise to swelling properties. The electrostatic repulsion between cationic particles on modified cellulose surface and the immobilization of the trapped interstitial water enables the creation of elastic structured zones of fibrillated agglomerates (Hubbe et al. 2017). The stable physical properties demonstrated by rheological measurements in Fig. 4 can accordingly be correlated to the high aspect ratio and specific surface

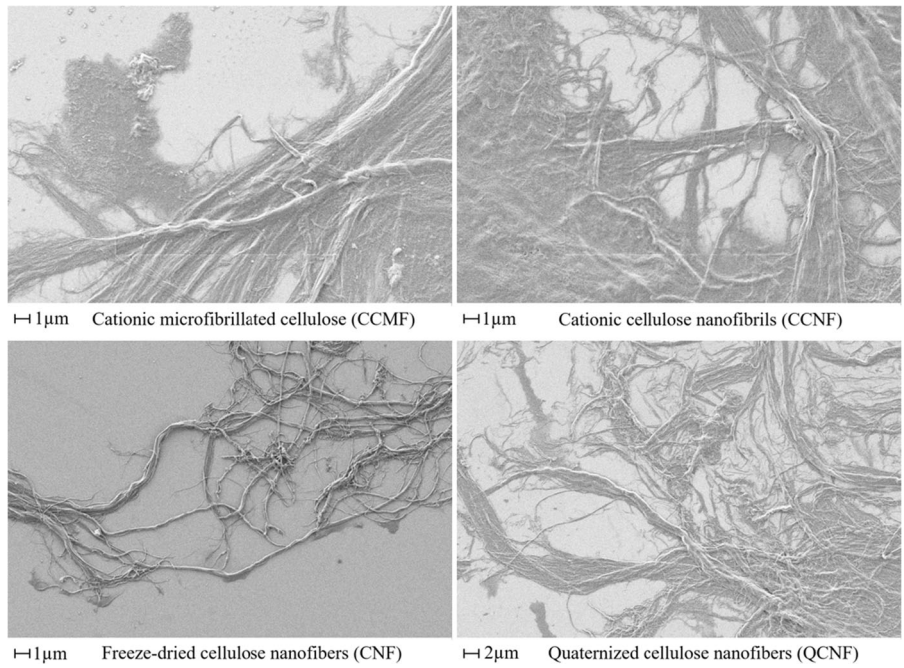

Fig. 5 SEM micrograph of freeze-dried water dispersions of CNFs, CCMFs, CCNFs and QCNFs

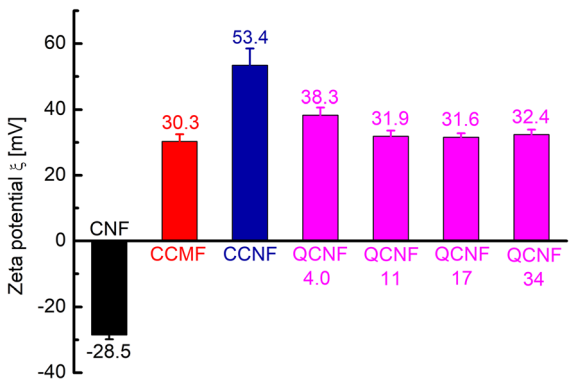

Fig. 6 Change in zeta potential ζ as a function of the of CNF, CCMF, CCNF and QCNF water dispersions

area, thus affecting the degree of entanglement of nanofibrils counterbalance and surpass the strong electrostatic repulsion of cationic cellulose.

Figure 6 illustrates the zeta potential of different cellulose samples. The zeta potential value of ±30 mV is considered optimum for the good stabilization of a nanodispersion (Freitas and Müller 1998). The original non-modified cellulose nanofibrils (CNFs) displayed negative zeta potential since the fibers possessed some carboxyl groups originating mainly from the residual hemicellulose in the pulp with a small amount attributable to cellulose oxidation during the pulping process (Olszewska et al. 2011; Sehaqui et al. 2015). The cationic modification changes the zeta potential to positive value due to the presence of TMA groups on the surface of the biopolymer as is evident in Fig. 6. Furthermore, the zeta potential is not a measure of the surface charge of the particles (not a function of TMA content). Regardless of the TMA content on the surface, the QCNF samples exhibited good stability with zeta potential on average being between 30 and 40 mV (see Fig. 6). A similar zeta potential value (30.3 mV) is exposed for cationically modified microfibrillated cellulose (CCMF). On the other hand, the increase of zeta potential value (53.4 mV) of commercial cationically modified nanofibrillated cellulose (CCNFs) is evident in Fig. 6. Finally, the difference in the zeta potential shown in Fig. 6 can be attributed to the difference between the raw materials. As reported in literature (Cinar Ciftci et al. 2020), industrial production of fibrillated cellulose results in wide fibril size distributions which effect the overall colloidal stability and rheological properties. CCNFs are better fibrillated than CNFs (mother material for cationization) as also morphologically significant difference (nanofiber diameter, aggregate adhesion, etc. …)

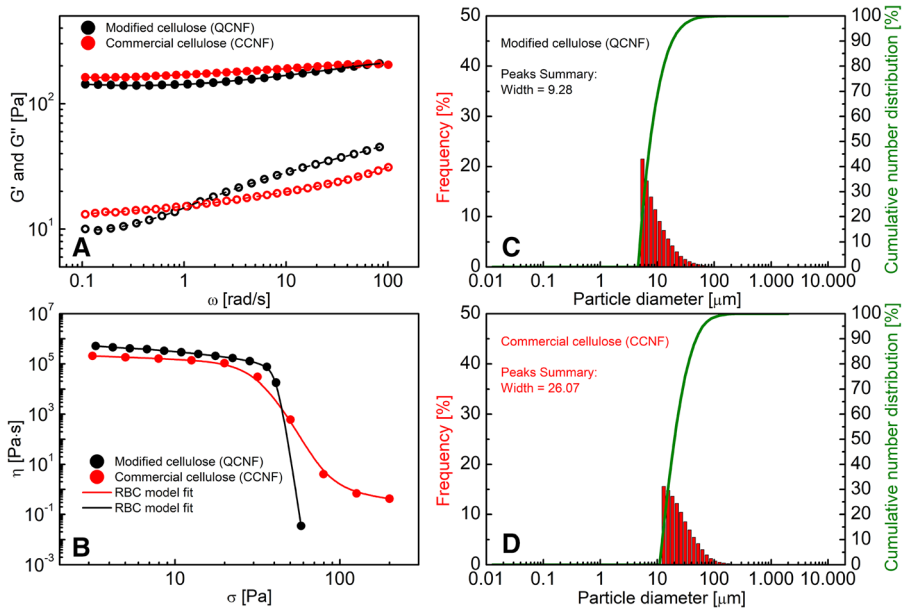

Fig. 7 Comparison of rheological properties (**A** and **B**) and number particle size distribution (**C** and **D**) for 2 wt% QCNFs (modified cellulose) with 2.1 mmol/g and 2 wt% CCNFs (commercial cellulose) with TMAC 2.24 mmol/g of TMAC on the surface of biopolymer, respectively. The mechanical spectrum (**A**) and flow curve (**B**) have already been presented in Figs. 3 and 4. In panel A, the filled and open symbols represent G' and G'', respectively

between both substances which has already been discussed in rheological and SEM characterization of materials. This could explain the difference in the results (rheological properties) shown in Tables 1 and 2 (see also Fig. 7 A and B) in cationic nanocellulose with the same biopolymer concentration and similar TMAC value. Therefore, it can be concluded that the rheological properties after quaternization foremost depend on the original cellulose materials.

The different types of cellulose fibers have completely different morphology which presents one of the major effects on rheological properties (Colson et al. 2016). The CCNFs have a less dense and less entangled network than QCNFs (Fig. 5). In the latter case, the fibrils created quite even blocks or segments structures which are a major contributor to the more viscoelastic and shear thinning character of QCNF than CCNF sample in similar TMAC and hydrogel concentration. The zeta potential (Fig. 6) has also shown that CCNFs are better fibrillated than QCNFs (higher zeta potential), it follows that well-dispersed individual nanoscale fillers can positively influence the increase in strength properties (Hubbe et al. 2017) which is more characteristic of gel-like systems than suspension of individual nanocellulose particles (Šebenik et al. 2019). For better comparison purposes, the more detailed presentation between the rheological properties of commercial (CCNFs) and modified (QCNFs) cationic CNFs are shown in Fig. 7 A and B. The mechanical spectrum (Fig. 7 A) shown a very similar curve for both samples presenting almost the same mechanical properties of CCNFs and QCNFs. Nevertheless, the differences between both samples can be attributed also to experimental error. The storage moduli values are practically the same and the small differences between loss moduli are illustrated between both CNFs. The slope of the loss modulus curve presents the less stable network structures. On the other hand, the flow behavior illustrated in Fig. 7B shows greater deviations between the observed samples. The slightly higher η_0 and σ_c (see also Tables 1 and 2) values can be observed for QCNFs. It has to be mentioned that it is difficult to experimentally determine the η_0 and σ_c values (depending on the type and rate of measurements) due to the fact that samples "creep" and are plastically deformed at very low shear stresses (η_0 is the value at zero shear stress). The narrow shear stress range where the viscosity decreases rapidly is the σ_c range. Therefore, the obvious difference between the CCNFs and QCNFs,

which can be related to the original material properties, is the range of the flow curve after σ_c. In Fig. 7B it is evident that QCNF flow curve has a more significant viscosity drop confined in a narrower shear stress interval than CCNFs. This effect is attributed to the different particle sizes of CCNF water dispersions. The highly complex network structure of QCNFs have more homogeneous agglomerates of nanocellulose fibers than CCNFs. The result is a faster arrangement of particles in the direction of shear action in the internal structure which it can be seen in narrower interval of viscosity drop (Fig. 7B). In the end, the differences between CCNFs and QCNFs are presented in the particle size analysis (Fig. 7 C and D) where the width of distribution is larger in QCNF sample. While detailed properties of original cellulose for quaternization of the commercial product are unknown, the synthesis route for CCNFs and QCNFs are the same, and the starting material was cellulose nanofibers with the forked structure of 50 nm in width and lengths of up to several hundred microns. Therefore, it could be speculated that the original material properties (which significantly affects the formation of agglomerates (Colson et al. 2016; Hubbe et al. 2017) play an important role in the rheological properties of the cellulose water dispersions also in this case. Additionally, the effect of NaOH concentration during synthesis should also be considered here. As already discussed in the introduction, the increase in alkali concentration allows penetration into the crystalline regions which resulted in a change in the dimension of the basic elementary cell and the formation of cellulose cellulose II.

Conclusions

In this study, the end properties of cationic micro- and nanofibrillated cellulose can be easily manipulated rather in the phase of molecule functionalization, the choice of micro- or nanofiber form, or both. The hypothesis of the optimal NaOH concentration in the quaternization of cellulose nanofibers was confirmed with the value of 0.152 of n_{NaOH}/n_{CNF}, calculated on the amount of dry polymer. At this point, the OH groups were in the most reactive form, which is why the addition of GTMAC to reach the desired concentration of cationic TMAC was optimized next. The TMAC concentration on QCNF surface was advanced to a maximum value of 3.3 mmol/g, which is, according to literature, the highest TMAC concentration to date. The content of cation groups on the polymer surface due to reflective electrostatic interactions significantly influences the viscoelastic behavior and shear thinning character of QCNF hydrogels. The GTMAC dependent zero-shear rate viscosity interval was determined between $13.5{\cdot}10^2 < \eta_{0\text{-}} < 1.03{\cdot}10^5$ [Pa·s] and the critical stress from $7.94 < \sigma_c < 103$ [Pa]. A broad range of parameters presents a great potential for the desired application based hydrogel preparation. In addition to the desired rheological properties, the biopolymer properties suitable for (ionic) crosslinking of the product can be designed by controlling the TMAC content, which has great utility in the drug delivery systems in controlled release technology. The equation to easy control and design desired TMAC content on the QCNF surface for future research was developed. Furthermore, a wide range of rheological properties of cationic nanocellulose has been expanded by a detailed study on the influence of different fiber size dimensions. Higher particle size and lower TMAC concentrations on microfibrillated cellulose influence the shear thinning behavior of hydrogels, which is reflected in higher values of zero-shear rate viscosity and critical stress. In the end, the SEM, zeta potential and particle size analysis confirmed that the rheological properties after quaternization are basically dependent on the morphology of original cellulose materials where the effect of NaOH concentration during synthesis plays important role in more homogeneity of the final product. Nevertheless, an accurate rheological study of quaternized micro- and nanofibrillated cellulose and the development of a model to easily control the desired rheological properties and the concentration of cationic groups during the quaternization of cellulose nanofibers allows the use of cellulose in many applications of cationic biopolymers. The effect of TMAC could have a major role in future research with the blends of (cationic and anionic) biopolymers, due to the crosslinking effect, swelling ability in various pH release environments, targeted drug delivery or in the case of adsorption of various molecules with negative charges on the surface.

Acknowledgment The authors acknowledge the financial support from the Slovenian Research Agency (research core funding No. P2-0191).

Authors' contributions Conceptualization: Tilen Kopač, Aleš Ručigaj; Methodology: Tilen Kopač; Formal analysis and investigation: Tilen Kopač, Aleš Ručigaj; Visualization: Tilen Kopač; Writing – original draft preparation: Tilen Kopač; Writing – review and editing: Matjaž Krajnc, Aleš Ručigaj; Funding acquisition: Matjaž Krajnc; Resources: Matjaž Krajnc; Supervision: Aleš Ručigaj.

Funding This work was supported by Slovenian Research Agency (Grant No. P2-0191).

Declarations

Conflict of interest The authors have no conflicts of interest to declare that are relevant to the content of this article.

Human or animals rights Authors declare no humans and/or animals were involved in this study.

References

Agoda-Tandjawa G, Durand S, Berot S et al (2010) Rheological characterization of microfibrillated cellulose suspensions after freezing. Carbohydr Polym 80:677–686. https://doi.org/10.1016/j.carbpol.2009.11.045

Ahmadi F, Oveisi Z, Samani M, Amoozgar Z (2015) Chitosan based hydrogels: characteristics and pharmaceutical applications. Res Pharm Sci 10:1–16

Ahmed EM (2015) Hydrogel: Preparation, characterization, and applications: a review. J Adv Res 6:105–121

Budtova T, Navard P (2016) Cellulose in NaOH–water based solvents: a review. Cellulose 23:5–55. https://doi.org/10.1007/s10570-015-0779-8

Caló E, Khutoryanskiy VV (2015) Biomedical applications of hydrogels: a review of patents and commercial products. Eur Polym J65:252–67

Chaker A, Boufi S (2015) Cationic nanofibrillar cellulose with high antibacterial properties. Carbohydr Polym 131:224–232. https://doi.org/10.1016/j.carbpol.2015.06.003

Cinar Ciftci G, Larsson PA, Riazanova AV et al (2020) Tailoring of rheological properties and structural polydispersity effects in microfibrillated cellulose suspensions. Cellulose 27:9227–9241. https://doi.org/10.1007/s10570-020-03438-6

Colson J, Bauer W, Mayr M et al (2016) Morphology and rheology of cellulose nanofibrils derived from mixtures of pulp fibres and papermaking fines. Cellulose 23:2439–2448. https://doi.org/10.1007/s10570-016-0987-x

Courtenay JC, Ramalhete SM, Skuze WJ et al (2018) Unravelling cationic cellulose nanofibril hydrogel structure: NMR spectroscopy and small angle neutron scattering analyses. Soft Matter 14:255–263. https://doi.org/10.1039/c7sm02113e

Dimic-Misic K, Puisto A, Paltakari J et al (2013) The influence of shear on the dewatering of high consistency nanofibrillated cellulose furnishes. Cellulose 20:1853–1864. https://doi.org/10.1007/s10570-013-9964-9

Ebhodaghe SO (2020) Hydrogel – based biopolymers for regenerative medicine applications: a critical review. Int J Polym Mater Polym Biomater 3:1–8. https://doi.org/10.1080/00914037.2020.1809409

Farshbaf M, Davaran S, Zarebkohan A et al (2017) Significant role of cationic polymers in drug delivery systems. Artif Cells, Nanomedicine, Biotechnol 46:1–20. https://doi.org/10.1080/21691401.2017.1395344

Freitas C, Müller RH (1998) Effect of light and temperature on zeta potential and physical stability in solid lipid nanoparticle (SLN®) dispersions. Int J Pharm 168:221–229. https://doi.org/10.1016/S0378-5173(98)00092-1

French AD (2017) Glucose, not cellobiose, is the repeating unit of cellulose and why that is important. Cellul 2017 2411 24:4605–4609. https://doi.org/10.1007/S10570-017-1450-3

Gasperini L, Mano JF, Reis RL (2014) Natural polymers for the microencapsulation of cells. J R Soc Interface 11(100):20140817

George A, Sanjay MR, Srisuk R et al (2020) A comprehensive review on chemical properties and applications of biopolymers and their composites. Int J Biol Macromol 154:329–338. https://doi.org/10.1016/j.ijbiomac.2020.03.120

Ghorbani S, Eyni H, Bazaz SR et al (2018) Hydrogels based on cellulose and its derivatives: applications, synthesis, and characteristics. Polym Sci - Ser A 60:707–722

Hasani M, Cranston ED, Westman G, Gray DG (2008) Cationic surface functionalization of cellulose nanocrystals. Soft Matter 4:2238–2244. https://doi.org/10.1039/b806789a

Ho TTT, Zimmermann T, Hauert R, Caseri W (2011) Preparation and characterization of cationic nanofibrillated cellulose from etherification and high-shear disintegration processes. Cellulose 18:1391–1406. https://doi.org/10.1007/s10570-011-9591-2

Hubbe MA, Tayeb P, Joyce M et al (2017) Rheology of nanocellulose-rich aqueous suspensions: a review. BioResources 12:9556–9661. https://doi.org/10.15376/biores.12.4.Hubbe

Iotti M, Gregersen ØW, Moe S, Lenes M (2011) Rheological studies of microfibrillar cellulose water dispersions. J Polym Environ 19:137–145. https://doi.org/10.1007/s10924-010-0248-2

Isogai A, Saito T, Fukuzumi H (2011) TEMPO-oxidized cellulose nanofibers. Nanoscale 3:71–85. https://doi.org/10.1039/c0nr00583e

Jacob J, Haponiuk JT, Thomas S, Gopi S (2018) Biopolymer based nanomaterials in drug delivery systems: a review. Mater Today Chem 9:43–55. https://doi.org/10.1016/j.mtchem.2018.05.002

John MJ, Thomas S (2008) Biofibres and biocomposites. Carbohydr Polym 71:343–364. https://doi.org/10.1016/j.carbpol.2007.05.040

Kaneko D, Thi Le NQ, Shimoda T, Kaneko T (2010) Preparation methods of alginate micro-hydrogel particles and evaluation of their electrophoresis behavior for possible

electronic paper ink application. Polym J 42:829–833. https://doi.org/10.1038/pj.2010.78
Kopač T, Krajnc M, Ručigaj A (2021) A mathematical model for pH-responsive ionically crosslinked TEMPO nanocellulose hydrogel design in drug delivery systems. Int J Biol Macromol 168:695–707. https://doi.org/10.1016/j.ijbiomac.2020.11.126
Kopač T, Ručigaj A, Krajnc M (2020) The mutual effect of the crosslinker and biopolymer concentration on the desired hydrogel properties. Int J Biol Macromol 159:557–569. https://doi.org/10.1016/j.ijbiomac.2020.05.088
Lee D, Oh Y, Yoo JK et al (2020) Rheological study of cellulose nanofiber disintegrated by a controlled high-intensity ultrasonication for a delicate nano-fibrillation. Cellulose 27:9257–9269. https://doi.org/10.1007/s10570-020-03410-4
Li J, Mooney DJ (2016) Designing hydrogels for controlled drug delivery. Nat Rev Mater 1:16071. https://doi.org/10.1038/natrevmats.2016.71
Lungu A, Cernencu AI, Dinescu S et al (2021) Nanocellulose-enriched hydrocolloid-based hydrogels designed using a Ca2+ free strategy based on citric acid. Mater Des 197:109200. https://doi.org/10.1016/j.matdes.2020.109200
Mittal A, Katahira R, Himmel ME, Johnson DK (2011) Effects of alkaline or liquid-ammonia treatment on crystalline cellulose: changes in crystalline structure and effects on enzymatic digestibility. Biotechnol Biofuels 4:41. https://doi.org/10.1186/1754-6834-4-41
Moberg T, Sahlin K, Yao K et al (2017) Rheological properties of nanocellulose suspensions: effects of fibril/particle dimensions and surface characteristics. Cellulose 24:2499–2510. https://doi.org/10.1007/s10570-017-1283-0
Nastaj J, Przewłocka A, Rajkowska-Myśliwiec M (2016) Biosorption of Ni(II), Pb(II) and Zn(II) on calcium alginate beads: equilibrium, kinetic and mechanism studies. Polish J Chem Technol 18:81–87. https://doi.org/10.1515/pjct-2016-0052
Olszewska A, Eronen P, Johansson LS et al (2011) The behaviour of cationic NanoFibrillar Cellulose in aqueous media. Cellulose 18:1213–1226. https://doi.org/10.1007/s10570-011-9577-0
Parhi R (2017) Cross-linked hydrogel for pharmaceutical applications: a review. Adv Pharm Bull 7:515–530. https://doi.org/10.15171/apb.2017.064
Peng N, Wang Y, Ye Q et al (2016) Biocompatible cellulose-based superabsorbent hydrogels with antimicrobial activity. Carbohydr Polym 137:59–64. https://doi.org/10.1016/j.carbpol.2015.10.057
Rebelo R, Fernandes M, Fangueiro R (2017) Biopolymers in medical implants: a brief review. Procedia Eng 200:236–243. https://doi.org/10.1016/j.proeng.2017.07.034
Salajková M, Berglund LA, Zhou Q (2012) Hydrophobic cellulose nanocrystals modified with quaternary ammonium salts. J Mater Chem 22:19798–19805. https://doi.org/10.1039/c2jm34355j
Samal SK, Dash M, Vlierberghe S, Van et al (2012) Cationic polymers and their therapeutic potential. Chem Soc Rev 41:7147–7194. https://doi.org/10.1039/c2cs35094g
Schenker M, Schoelkopf J, Gane P, Mangin P (2019) Rheology of microfibrillated cellulose (MFC) suspensions: influence of the degree of fibrillation and residual fibre content on flow and viscoelastic properties. Cellulose 26:845–860. https://doi.org/10.1007/s10570-018-2117-4
Šebenik U, Krajnc M, Alič B, Lapasin R (2019) Ageing of aqueous TEMPO-oxidized nanofibrillated cellulose dispersions: a rheological study. Cellulose 26:917–931. https://doi.org/10.1007/s10570-018-2128-1
Šebenik U, Lapasin R, Krajnc M (2020) Rheology of aqueous dispersions of Laponite and TEMPO-oxidized nanofibrillated cellulose. Carbohydr Polym 240:116330. https://doi.org/10.1016/j.carbpol.2020.116330
Sehaqui H, De Perez U, Tingaut P, Zimmermann T (2015) Humic acid adsorption onto cationic cellulose nanofibers for bioinspired removal of copper(ii) and a positively charged dye. Soft Matter 11:5294–5300. https://doi.org/10.1039/c5sm00566c
Siqueira P, Siqueira É, De Elza A et al (2019) Three-dimensional stable alginate-nanocellulose gels for biomedical applications: towards tunable mechanical properties and cell growing. Nanomaterials 9:78. https://doi.org/10.3390/nano9010078
Spaic M, Small DP, Cook JR, Wan W (2014) Characterization of anionic and cationic functionalized bacterial cellulose nanofibres for controlled release applications. Cellulose 21:1529–1540. https://doi.org/10.1007/s10570-014-0174-x
Tang Y, Wang X, Huang B et al (2018) Effect of cationic surface modification on the rheological behavior and microstructure of nanocrystalline cellulose. Polymers (Basel) 10:278. https://doi.org/10.3390/polym10030278
Tavakoli J, Tang Y (2017) Hydrogel based sensors for biomedical applications: an updated review. Polymers (Basel) 9:364. https://doi.org/10.3390/polym9080364
Turpeinen T, Jäsberg A, Haavisto S et al (2020) Pipe rheology of microfibrillated cellulose suspensions. Cellulose 27:141–156. https://doi.org/10.1007/s10570-019-02784-4
Udoetok IA, Wilson LD, Headley JV (2016) Quaternized cellulose hydrogels as sorbent materials and pickering emulsion stabilizing agents. Materials. 9(8):645. https://doi.org/10.3390/ma9080645
Velema J, Kaplan D (2006) Biopolymer-based biomaterials as scaffolds for tissue engineering. Adv Biochem Eng Biotechnol 102:187–238. https://doi.org/10.1007/10_013
Wang X, Chang CH, Jiang J et al (2019) The crystallinity and aspect ratio of cellulose nanomaterials determine their pro-Inflammatory and immune adjuvant effects in vitro and in vivo. Small 15:1901642. https://doi.org/10.1002/smll.201901642
Zaman M, Xiao H, Chibante F, Ni Y (2012) Synthesis and characterization of cationically modified nanocrystalline cellulose. Carbohydr Polym 89:163–170. https://doi.org/10.1016/j.carbpol.2012.02.066

Zhang W, Zhang Y, Lu C, Deng Y (2012) Aerogels from crosslinked cellulose nano/micro-fibrils and their fast shape recovery property in water. J Mater Chem 22:11642–11650. https://doi.org/10.1039/c2jm30688c